

Chapter 9: Experimental Methods

A model of actuator behavior is derived in the previous chapter. The task is now to compare actuator response with model predictions. The apparatus and methods employed are described in this chapter and the results presented in Chapter 10. The procedures are very similar to those employed in Chapter 5, except that swept sine voltage inputs are used instead of stepped potential or current. Polypyrrole films are held under isotonic conditions (constant force). The admittance, and strain to current transfer functions are measured. With the film at constant length (isometric) the stress to current transfer function is recorded. The modeled transfer functions are fit to the data to obtain estimates of the diffusion coefficient and the strain to charge ratio. Electromechanical efficiency is calculated from the data and compared with theory.

Section 9.1 provides a general discussion of types of signals employed to measure transfer functions of dynamically linear systems, explaining why swept sine analysis is chosen. The sections that follow describe the experimental apparatus in detail and the measurement procedures. Figure 1 is a diagram of the entire apparatus, whose components are summarized at the beginning of Section 9.2.

9.1 Advantages and Disadvantages of Swept Sine Analysis

A number of standard waveforms are used in linear system identification, including impulses, steps, white noise, pseudo-random binary sequences, and swept-sine. The type of signal used is justified on the basis of measurement time, noise levels, the need to determine the extent non-linearities and convenience.

Figure 1

Swept sine analysis has several advantages. Sine waves are a natural choice of waveform, since they are eigenfunctions of every linear equation. Thus, if a system is linear, a sinusoidal input will result in a sinusoidal output of the same frequency, but shifted in amplitude and phase. This allows noise and non-linearities to be readily identified given the power spectra of the input, G_{11} and output, G_{22} and the cross-spectrum, G_{12} via the coherence squared function, γ^2 :

$$\gamma^2(f) = \frac{\text{Re}(G_{12}(f))^2 + \text{Im}(G_{12}(f))^2}{G_{11}(f) \cdot G_{22}(f)}. \quad 1$$

The portion of the coherence squared due to uncorrelated noise is identified by averaging, enabling the extent of non-linearities, appearing for example as harmonics of the input frequency, to be identified.

Scaling between input and output is a characteristic of all linear systems. If a system is linear the scaling of inputs of any form must lead to an output whose magnitude is changed by the same factor. Usually the range over which scaling applies is limited, either by the system, or the measuring device, and these limits may be a function of frequency. Sine wave analysis allows the input signal to be maximized at every frequency such that signal to noise levels can be maximized. Similarly, measurement of the output can be optimized at each frequency by, for example, using auto-ranging on the analog to digital converters, as is done in obtaining some of the frequency response data presented in Chapter 10.

A further advantage of swept sine analysis is that the frequency intervals are readily chosen. In the experiments presented here, a logarithmic frequency scale is used.

Figure 2a

Figure 2b

The primary disadvantage of swept sine analysis is the length of each measurement, particularly if high frequency resolution and spacing is required at low frequencies. If the system under test exhibits time-dependent behavior, then swept sine analysis may in fact be unusable. The speed disadvantage is compensated for by the fact that commercial instruments are available to automate swept sine system identification.

Swept sine analysis has thus been chosen for this study because it enables ready identification of noise and non-linearities, maximization of signal to noise as a function of frequency, and ready use of a logarithmic frequency scale.

9.2 Description of the Apparatus

The aim is to measure the impedance, strain to charge, and stress to charge transfer functions of polypyrrole films. These experimental results will then be compared to model predictions. The impedance measurements are performed with the film held at constant force and bathed in electrolyte. Swept sine potentials are applied to the film relative to a reference electrode, and the resulting current is recorded. During the strain to charge and stress to charge measurements, a swept sine voltage is applied to the film, and current is recorded, as is either strain or stress. In the stress to charge case, the film is held at constant length (isometric), while the strain to charge is performed under isotonic conditions. A block diagram of the apparatus is shown in Figure 1, a photo of the electrochemical-mechanical cell is shown in Figure 2 and the electrical circuit diagram is shown in Figure 3. The apparatus consists of:

Figure 3

- the cell, comprising of a bath in which the polymer film is tested, including clamps to mechanically and electrically contact the film, a counter electrode, and a reference electrode;
- a potentiostat for applying potentials to the film relative to a reference electrode;
- a load cell and amplifier for measuring force on the film;
- a stepping motor, motor controller and linear stage for applying displacements to the polymer film;
- a data acquisition card including an analog to digital (A/D) channel used to input the force to a computer, and a digital output used to send step and direction commands to the stepper motor;
- a computer running a custom Java application, that reads in force levels and outputs motor displacement commands so as to maintain constant force on the film (isotonic mode) or measure the polymer stress/strain curve;
- a dynamic signal analyzer (HP3562A) that outputs swept sine waves, measures the system response, and computes the transfer functions; and
- a second computer that interfaces to the HP3562A, and which, via software, controls the frequency range, resolution and other features of the transfer function measurement, and records the output data.

The subcomponents of the apparatus are now described in detail, followed by a description of the experimental procedures.

9.2.1 The Electrochemical-Mechanical Cell

Figure 2 shows the bath in which electrical and mechanical tests are performed on polypyrrole films. The bath is the electrochemical cell, including the polymer/working electrode, a reference electrode and a counter electrode, immersed in electrolyte. It is also the mechanical test platform, including a load cell that measures force applied to the film, clamps through which force is transmitted, and a shaft by which displacements are applied. The bath is bolted to a stainless steel optical table, which sits on air bearings to provide vibration isolation.

9.2.1.1 The Nylon Bath

The bath itself is a nylon block (50 mm high \times 160 mm long \times 90 mm wide), as seen in Figure 2, into which a 40 mm deep, 70 mm wide and 140 mm long well has been machined. The nylon bath is bolted to the optical table at the four corners. It serves to contain the liquid electrolyte in which the polypyrrole film is immersed.

9.2.1.2 Electrical and Mechanical Contact with the Polypyrrole Film

Polypyrrole films are clamped at either end within the bath, as shown in Figure 2. Electrical and mechanical contact is made via the two clamps, which have vertical slots into which the film is placed. The clamps are polyacetal, 40 mm high, 20 mm wide, parallel to the film, and 15 mm thick. In fact the 15 mm thick section consists of two, 7.5 mm thick pieces that are bolted together using stainless steel M3 screws. The polymer films are sandwiched between the plates. Platinum coated stainless steel sheet is also placed within the slots to provide electrical contact with the polymer. A stainless steel

M3 screw is threaded vertically into each clamp to electrically contact each stainless steel sheet.

Two 6.31 mm diameter solid aluminum shafts transmit force beyond the bath. One shaft is 35 mm long, and connects with a load cell, described below, and then on to an aluminum L-bracket (6 mm thick \times 100 mm high \times 50 mm wide) that is bolted to the underlying optical table. The second shaft, visible in Figure 2, is used to impart displacement. It is 145 mm long, and is bolted to the linear displacement stage.

9.2.1.3 The Reference Electrode

Either aqueous calomel, as shown in Figure 2, or a silver/silver perchlorate reference electrode is placed next to the film.

The glass body, silver wire, tetrafluoroethylene cap and Vycor® (www.corning.com) plug of the Ag/AgClO₄ reference are purchased from Bioanalytical Systems, www.bioanalytical.com (MF-2062 Non-aqueous ref kit). The glass tube is 5.6 mm in outer diameter, 80 mm long, and tapers at the bottom to a 4 mm diameter Vycor® plug, fixed on with heat shrink tubing. A 60 mm long, 500 μ m diameter silver wire is centered within the glass body via a polytetrafluoroethylene cap. The silver wire is soldered to a brass pin, to which a coaxial cable is in turn soldered. The coaxial cable is connected to the reference electrode port on the potentiostat. The glass tube is filled with 0.01 M AgClO₄ and 0.05 M (C₂H₅)₄N ClO₄ in propylene carbonate, following the methods of Courtot-Coupez and L'Her (Courtot-Coupez and L'Her 1970). The Ag/Ag⁺ reference is measured to sit at a potential of 0.716 V vs. a standard aqueous calomel reference at room temperature.

The calomel electrode (Accumet model 13-620-79, www.fisherscientific.com), has a glass body 10 mm in diameter, and 42 mm long. The tip has a 1.3 mm diameter porous ceramic plug.

The three key properties of a reference electrode are its stability, accuracy and impedance. The impedances of the calomel and the Ag/AgClO₄ references are shown in Figures 4 and 5, as measured using an HP 4194A impedance analyzer. Stability and accuracy are judged in two ways. Two Ag/AgClO₄ reference electrodes are used during the initial experiments, enabling the two references to be compared. They remain within 5 mV over a period of several days. Also, once every 48 hours, the reference potential is compared with that of the calomel reference. The values remain within 10 mV. Such stability proves to be ample given that the impedance and strain to charge are dynamically linear over a range of at least ± 0.5 V. The calomel electrode experiences significant salt draining when immersed in propylene carbonate-based electrolytes for more than 20 hours. Its much lower impedance proves useful in making accurate high frequency measurements, and therefore it is used for some measurements over periods of several hours, after which the saturated potassium solution is replenished.

9.2.1.4 The Counter Electrode

Two 100 mm \times 100 mm glassy carbon plates, one of which is shown in Figure 2, are employed as the counter electrodes. They are placed 65 mm apart, symmetrically about the clamped film, with the bottom 35 mm immersed in electrolyte. The symmetrical placement is important to ensure that nearly equal currents flow in either side of the polypyrrole film.

Figure 4

Figure 5

9.2.1.5 The Electrolyte

The electrolyte is 0.05 M, 0.3 M, or 0.37 M tetraethylammonium hexafluorophosphate (Aldrich 43,411-6, 99% pure, www.aldrich.com) in propylene carbonate (Aldrich, 31,032-8, 99.7 %, packed under N₂), unless otherwise noted. Both reagents are used as shipped, and employed immediately after opening. Nitrogen is bubbled through the solution before use. The electrolyte is chosen because it produces very low background currents (Bard and Faulkner 1980), thereby minimizing parasitic reactions. Also, it employs the same electrolyte and dopants used during synthesis, thereby minimizing the number of variables.

9.2.1.6 The Film under Test

Polypyrrole films doped with hexafluorophosphate anions and grown as described in Chapter 4 are tested. They are cut into strips of between 50 mm and 80 mm in length, and between 2 mm and 10 mm in width. Film thicknesses range from $8.5 \pm 2 \mu\text{m}$ to $51 \pm 3 \mu\text{m}$. Polypyrrole films synthesized in this manner are used because of their outstanding conductivity* (up to $4.5 \times 10^4 \text{ S} \cdot \text{m}^{-1}$), large strain to charge ratio ($\sim 1.5 \times 10^{-10} \text{ m}^3 \cdot \text{C}^{-1}$), and relatively high tensile strength (30 to 70 MPa).

9.2.1.7 Nitrogen Atmosphere

Experiments are performed under a nitrogen atmosphere. A positive pressure of nitrogen gas is maintained within a 50 mm long \times 26 mm wide \times 31 mm high glass enclosure.

* Polypyrrole films synthesized in this manner are exceeded in conductivity amongst polymers at room temperature only by polyacetylene, which is unstable (Kohlman and Epstein 1998).

9.2.2 The Dynamic Signal Analyzer

The HP3562A Dynamic Signal Analyzer (DSA) (www.agilent.com) provides a logarithmic swept sine voltage output to the potentiostat, and records the resulting current to voltage transfer function (admittance), current to strain, or current to stress. The circuit used to record admittance is shown in Figure 3. The frequency range employed is 100 μ Hz to 100 kHz. The input impedance is 1 M Ω and < 100 pF. Each input has a common mode rejection ratio of 10^{-4} . A 14 bit auto-ranging A/D samples the inputs at 256 kHz. The inputs are digitally filtered and fast Fourier transformed (FFT). The power spectrum of channels 1 and 2, G_{11} and G_{22} , are found by multiplying the Fourier transformed data by their complex conjugates. The cross-power spectrum, G_{12} , is calculated by multiplying the FFT of input 1 by the complex conjugate of the FFT of input 2. During a swept sine measurement, the HP3562A outputs frequency, f , channel 1 power spectrum, $G_{11}(f)$, channel 2 power spectrum $G_{22}(f)$, the real part of the cross-spectrum, $\text{Re}(G_{12}(f))$ and the imaginary part of the cross-spectrum, $\text{Im}(G_{12}(f))$ from which the transfer function, $H(f)$ and variation accounted for $\gamma^2(f)$ functions are calculated:

$$|H(f)| = \frac{\sqrt{\text{Re}(G_{12})^2 + \text{Im}(G_{12})^2}}{G_{11}}, \quad 2$$

$$\angle H(f) = \arctan\left(\frac{\text{Im}(G_{12})}{\text{Re}(G_{12})}\right), \quad 3$$

$$\gamma^2(f) = \frac{\text{Re}(G_{12})^2 + \text{Im}(G_{12})^2}{G_{11} \cdot G_{22}}. \quad 4$$

The accuracy in phase is $\pm 2.5^\circ$ per channel, and in magnitude is determined by the 14 bit A/D, plus an additional uncertainty of 0.025% of input range. The DSA auto-ranges

down to ± 10 mV full scale. Frequency response channel matches are specified to be within ± 0.1 dB and $\pm 0.5^\circ$. Auto-ranging is used in the experiments presented down to a frequency of ~ 20 mHz. At lower frequencies it becomes very slow, and ranging is performed manually, keeping signal level above $\frac{1}{2}$ of the input range where possible.

In order to perform swept sine analysis using the HP3562A a number of parameters must be specified, including the frequency range, input amplitude, frequency resolution, and number of averages. In the experiments that follow these are provided to the HP3562A DSA via IEEE 488 link with a PC, as now described.

Figure 6

Figure 7

Figure 8

9.2.3 The Dynamic Signal Analyzer: Settings and Data Retrieval

Measurement parameters are uploaded to the HP3562A from a notebook PC (IBM iSeries 2611-552, Running Windows 98, www.ibm.com) via an IEEE 488 interface (National Instruments NI488-2 PCM-CIA to GPIB card, www.natinst.com). This is done via HP VEE 5.0, (www.agilent.com) the Hewlett Packard/Agilent Technologies visual programming language designed to control interactions between computers and instruments for measurement, data analysis and data storage.

The program is shown in Figures 6, 7 and 8. Figure 6 shows the overall flow diagram of the program, with the blocks titled HP3562A indicating interactions with the DSA. Figures 7 and 8 show the commands of code used to set up the DSA for measurement, found in the HP3562A block at the top right of Figure 7, and the code used to write to file, bottom right. Start and stop frequencies, the number of data points per decade, the number of averages, and the peak signal level are all specified by the user in the text boxes at the top left. These are input to the HP3562A, which is set for logarithmic swept sine frequency response measurement with auto-ranging and so on, as shown in Figure 7. The command is also given to start measuring frequency response.

As data are collected and computed for each point in the frequency scan (f , G_{11} , G_{22} , $\text{Re}(G_{12})$, $\text{Im}(G_{12})$), they are stored in a buffer on the HP3562A, ready for transmission to the computer. The total number of data points to be output is computed (Number of Counts Box), and a loop is started in which one data point is collected for each cycle, the total number being displayed in the For Count box. A cycle is completed when a break is reached. The break occurs when data are read (lower right HP3562A box). First however, the program checks every 0.2 s to see if new data from the next measured

frequency is ready. If new data are ready then gain, $|H|$, phase, $\angle H$, frequency, f , and coherence squared, γ^2 , are written to file, with computations being done as explained in the previous section, using the relationships: $f \Leftrightarrow x[4]$, $G_{11} \Leftrightarrow x[0]$, $G_{22} \Leftrightarrow x[1]$, $\text{Re}(G_{12}) \Leftrightarrow x[2]$, and $\text{Im}(G_{12}) \Leftrightarrow x[3]$. The data obtained are then read by Mathcad 2000 Professional (www.mathsoft.com), where they are plotted and manipulated.

9.2.4 The Potentiostat

A potentiostat applies current between the working electrode (polymer film) and the counter electrode such that the working to reference electrode voltage difference matches an input command potential. The potentiostat circuit employed is shown in Figure 3, and is similar to circuits described by Bard and Faulkner (Bard and Faulkner 1980). It includes an adder, such that two inputs (e.g. swept sine and an equilibrium offset) can be summed, and, to improve reference voltage stability, a current buffer. The voltage drop across a resistor, R_i , in series with the output, is used to measure current, and applied work to reference voltage is measured at the output of the current buffer.

Some key properties of a potentiostat are the maximum voltage and current that can be output, how well and over what bandwidth the output potential matches the command voltage, and the accuracy of electric current measurement. Essentially, the potentiostat has a bandwidth of 100 kHz, a maximum output current of 1 A, and a cell potential range of ± 20 V. However, these properties are functions of the cell impedance, the impedance of the current measuring device, and the extent of any parasitic capacitances to ground as now discussed in detail. Equations are developed that successfully predict response as a

function of cell impedances, parasitic impedances and measurement device properties, as listed in Figure 9. Skip to Section 9.2.4.3 for a brief summary.

9.2.4.1 Limits on Potentiostat Current and Voltage Output

The maximum work to reference voltage, V_o , that can be generated is a function of either the maximum voltage output of the power amplifier or its maximum current, at a given frequency. It is also a function of the test cell impedances, Z_w and Z_c , and the size of the current measuring resistor, R_i , shown in Figure 3. Z_w , Z_c and Z_r represent reference to working electrode, counter to reference, and electrolyte to reference impedances, respectively, as shown in Figure 3. The product of the peak output current and the test cell's work to reference impedance, Z_w , provides one limit on maximum output voltage. The second limit on peak work to reference voltage, V_o , is determined by the product of the maximum output voltage and the ratio of Z_w to the sum of the real parts of R_i , Z_w and Z_c :

$$V_o^{max} = V_{max} \cdot \left| \frac{Z_w}{R_i + Z_w + Z_c} \right|. \quad 5$$

The maximum cell voltage and current are determined by the performance of the PA07 power operational amplifier (Apex, Tucson, AZ, USA), which can output a maximum of ± 45 V and ± 5 A. However, in the experiments conducted here, an HP E3631A triple output DC power supply provides ± 25 V to the PA07 and is current limited to ± 1 A, so that the maximum PA07 output is ± 20 V, and ± 1 A. The maximum voltage output, V_M , drops at frequencies above 15 kHz, to $V_M = \pm 6$ V at 100 kHz. Thus, in order to follow an input, V_i , up to 100 kHz, two conditions must be met. Firstly, the current must be high enough to generate the desired voltage drop. The magnitude of the product of maximum

Figure 9

current, I_M , available and the work to reference impedance, must be greater than the desired voltage, V_i : $|Z_w| \cdot I_M > V_i$, so that $|Z_w| > V_i / 1.0 \text{ Amp}$. Secondly, the available voltage must be high enough to generate the desired voltage drop between the working and reference electrodes, creating the condition: $|R_i + Z_w + Z_c| \cdot 6 \text{ Volts} > |Z_w| \cdot V_i$.

9.2.4.2 Potentiostat Voltage Tracking, Current and Admittance Measurement

Ideally the output work to reference voltage, V_o , is equal in amplitude and phase to the input voltage, V_i , and the current is simply $I = Z_w \cdot V_i^{-1}$. Assuming that the op amp outputs are not being saturated, there are six primary sources of error:

1. The gains of the operational amplifiers are finite;
2. Bias currents create offsets in the applied potential;
3. Input impedance and common mode rejection ratios (CMRR) of the voltage measuring devices are finite;
4. Stray capacitances lead to an overestimate of current;
5. Offsets arise due to differences in resistance between R_1 , R_2 and R_3 used in the adder portion of the circuit shown in Figure 3;
6. There are sources of noise, both internal (e.g. thermal noise) and external (e.g. 60 Hz coupling).

These factors are now considered, and their predicted effects used to explain the ratio of measured to command voltages (Figure 10), measured vs. actual currents (Figure 11), and measured vs. predicted admittance (Figure 12). In performing the characterization, a test circuit is chosen whose impedances are similar in magnitude to those expected in the real

Figure 10

Figure 11

Figure 12

test cell, with $Z_w=20.1 \Omega+(j\cdot\omega\cdot94.3\mu F)^{-1}$, $Z_c=100.46 \Omega$, $R_i=99.6 \Omega$ and $Z_r=102.68 \text{ k}\Omega$.

The circuit is tested using short leads and again using the same electrical connections used in making contact with the electrochemical bath. In all cases $\pm 0.4 \text{ V}$ swept sine inputs were applied using the HP3542A Dynamic Signal Analyzer, connected as depicted in Figure 3, which also measures and computes the current to voltage transfer function.

Figure 10 shows the ratio of actual work to reference voltage, V_o , to command input, V_i . Figure 11 shows the ratio of current through the working electrode to current through R_i , and Figure 12 depicts the measured admittance. All measurements, represented by the blue dots, are taken using the test circuit with the leads and connectors used in the electrochemical test cell. The red lines are model predictions, accounting for finite gains, input impedances and parasitic capacitances. These equations are listed in Figure 9, along with the equivalent circuit used to obtain them. The influence of the various sources of offset and error are now discussed.

9.2.4.2.1 Effect of Finite Operational Amplifier Gain

The operation amplifier gains are functions of frequency, as given in their specification sheets (www.lineartechnology.com, and www.apexmicrotech.com). At a given frequency, the Apex PA07 has a gain of G_p , and the LT1028 has a gain of G_b . Inspection of the circuit diagram, Figures 3 and 9, leads to a relationship between the output voltage, V_o , and input voltage, V_i :

$$\frac{V_o}{V_i} = \frac{G_p}{\frac{G_p \cdot G_b}{(1 + G_b)} + \frac{2 \cdot (R_i + Z_c + Z_w)}{Z_w}}, \quad 6$$

where Z_r , Z_c , and Z_w are the reference, counter and working electrode impedances of the cell under test. As G_p and G_b tend to infinity, the output, V_o , approaches the magnitude and phase of the input, V_i .

Measured values of V_i/V_o and those predicted by Equation 6* are plotted in Figure 10. Note that the actual voltage is less than half the command potential at 100 kHz. In cases where the precise magnitude of the applied voltage is important, this effect must be compensated for at frequencies of greater than 10 kHz. Providing that the system being tested is dynamically linear, the increased output voltage will be compensated by an increased current, thereby leaving the gain and phase unaffected, as is observed in the admittance data of Figure 12.

9.2.4.2.2 Offsets due to Bias Currents

The operational amplifier inputs act as current sources or sinks, producing bias currents, I_b . In the PA07 this current is 50 pA at most (www.apexmicrotech.com), while in the LT1028 it is typically 30 nA and can reach 100 nA (www.lineartechnology.com). The PA07 bias produces a negligible voltage offset through the 10 k Ω resistors. The LT1028 bias current drops across the reference electrode, creating an offset of $Z_r \cdot I_b$. Given the Ag/AgClO₄ reference electrode has an impedance of $7 \cdot 10^4 \Omega$, the offset is less than 7 mV. The bias current will also create a potential drop between the reference electrode and the working electrode, and increase the actual current to the working electrode by its

* The LT1028 voltage gain is $3 \cdot 10^7$ at frequencies below 1 Hz. At higher frequencies the log gain has a slope of -1 with log frequency, dropping one decade for every decade in frequency, up to 100 kHz. The gain at 100 kHz is $G_b=1000$. The PA07 gain is 10^5 below 10 Hz, and drops off with a slope of -1 , so that at 100 kHz the gain is $G_p=10$. The phase is -90 degrees between 100 Hz and 100 kHz, as confirmed by measuring the small signal frequency response. See data sheets (www.lineartechnology.com, www.apexmicrotech.com).

value. This has a negligible effect unless high work to reference impedances or very low applied potentials are used.

9.2.4.2.3 Effects of Stray Capacitances

Stray capacitance provides parallel paths to ground, as shown in Figure 12, represented by admittances Y_p^{-1} and Y_{pr}^{-1} , and in Figure 3 by C_{si} and C_{sv} . They often result from wires passing close to a ground plane, grounded coaxial cables ($\sim 90 \text{ pF}\cdot\text{m}^{-1}$), grounded connectors ($\sim 0.06 \text{ pF}$ coax to BNC) and finite input impedances. There are two points in the circuit at which stray capacitance can compromise potentiostat performance. Parasitic capacitance occurring at points between the working electrode and the current measuring resistor, R_i , provides an alternate current path to ground, so that the actual current to the working electrode is less than the measured current. The effect on current measurement for a capacitance, C_{si} , is negligible providing:

$$Z_c + Z_w \ll \frac{I}{j \cdot \omega \cdot C_{si}} . \quad 7$$

The effect of stray capacitance increases with frequency. Stray capacitance between the reference electrode and the input to the LT1028 can cause offsets in both the measured voltage and current. This stray capacitance acts along with the reference electrode to form a voltage divider, correspondingly reducing the measured voltage. The offset is avoided providing that:

$$Z_r \ll \frac{I}{j \cdot \omega \cdot C_{sv}} . \quad 8$$

If the reference electrode impedance is comparable in magnitude to the working electrode impedance, then a significant portion of the current can leak through the

reference. This can be a problem if a current buffer is not used, or stray capacitance reduces the effective reference impedance.

Figure 11 shows the ratio of ‘actual’ to measured currents in the test circuit. The measured current, I_{rd} in Figure 9, is measured across R_i , while the ‘actual’ current is measured across the $20.1\ \Omega$ test circuit resistor that forms part of Z_w . Equation 7 allows the determination of an upper bound on this parasitic capacitance, and suggests that $C_{si} < 200\ \text{pF}$. Deviation at low frequencies is a result of the finite common mode rejection ratio of the DSA, as discussed in the section that follows.

Stray capacitance between the reference electrode and the current buffer, C_{sv} in Figure 3, creates a voltage divider. Since the work to reference voltage is measured at the current buffer output, the voltage is underestimated if the reference admittance is large relative to the magnitude of the capacitor admittance, $\omega \cdot C_{sv}$. This effect results in a rise in admittance gain and phase at high frequency. Figure 12, depicting the test cell admittance, shows slight increases at frequencies above 10 kHz, where the test cell is expected to show a purely resistive response, given that the frequency is well above the $R \cdot C$ time constant. These offsets are the result of stray capacitances in the grounded coaxial cable connector, measured to be 100 pF. The red curves in Figure 12 are model predictions, using the equations in Figure 9, which include the effect of coaxial connector capacitance and finite gain. The model and observations agree, suggesting that parasitic impedances can be accounted for, providing the magnitude of the capacitance is known. The same connectors used in the test circuit measurement are employed in the electrochemical cell, and again are found to be the primary source of stray capacitance. Thus the stray capacitance can be accounted for in interpreting polymer admittance data.

9.2.4.2.4 Effect of Finite Voltage Measuring Input Impedances and Common Mode Rejection Ratios

In order to measure small currents, it is tempting to increase the size of the current measuring resistor, R_i , shown in Figure 3. This leads to measurement errors if the input impedance of the measuring device becomes significant relative to R_i^{-1} . Input impedance is generally characterized by a capacitance, C_{in} , in parallel with a resistance, R_{in} , as in Figure 3, in which the input impedances to the DSA are shown. The maximum value of R_i for a given acceptable error, e , in current measurement is determined by:

$$R_i < e \cdot R_{in}, R_i < \frac{e}{\omega_{max} \cdot C_{Input}}. \quad 9$$

R_i should not exceed 150 Ω to ensure an offset of less than 1% at 100 kHz when the DSA ($C_{in} < 100$ pF) is employed to measure current. Instrumentation amplifiers are used to isolate the circuit from the DSA input if higher current sensitivities are required.

A second source of error is the finite common mode rejection ratio (CMRR) of the inputs. Since the current measurement is not taken with respect to ground, the common mode is often a significant fraction of the applied potential. The error in the measurement of current magnitude, e_{CMRR} , for a given common mode voltage, V , and current, I , is:

$$e_{CMRR} = \frac{V \cdot CMRR}{I \cdot R_i} \leq \frac{CMRR \cdot V}{|Y| \cdot V_i \cdot R_i} = \frac{CMRR \cdot (Z_w + Z_c + R_i)}{|Y| \cdot R_i \cdot Z_w}. \quad 10$$

The DSA CMRR is 10^{-4} , and explains the deviation from the expected behavior below 100 mHz observed in Figures 11 and 12. The CMRR offset is largest when impedance is high and currents are small. The effects of common mode rejection ratio and finite

measurement device input impedance are readily determined and modeled, allowing them to be distinguished from the electrochemical cell response.

9.2.4.2.5 Amplitude Offset due to Resistor Mismatch

If the resistors R_1 , R_2 , and R_3 , used in the adder portion of the circuit shown in Figure 3, are not perfectly matched, the output voltage, V_o , will differ from the desired input voltage, V_i , and the second input, V_{eq} , according to the equations:

$$V_o = V_{eq} \cdot \frac{R_3}{R_1} + V_i \cdot \frac{R_3}{R_2} . \quad 11$$

The carbon resistors are selected to match within 0.5 %, leading to correspondingly small offsets.

9.2.4.2.6 Noise

The use of swept sine analysis enables signal to noise levels to be readily identified via the coherence squared (γ^2), Equation 4. The coherence squared is consistently above 0.99 from 0.1 mHz to 100 kHz in measurements of the admittance transfer function. Measurements of strain and stress to current transfer functions are limited by noise. Averaging of up to 1000 samples per frequency is used in these measurements. The measured γ^2 associated with these data are presented in Chapter 10.

9.2.4.3 Summary of Potentiostat Properties

The potentiostat is capable of voltage outputs of up to ± 20 V and currents as high as ± 1 A. The power supplies used limit these maxima. The accuracy with which measurements are made depends on frequency, load, measuring device input impedance, common mode rejection, and the magnitudes of parasitic impedances. Equations which

account for the finite gains of the operational amplifiers, the impedances of the test circuit and the parasitic impedances, are given in Figure 9, enabling these factors to be compensated for in analyzing measured admittance data.

9.2.5 Load Cells and Amplifier

Two load cells are employed to measure force on the polymer film, the choice of load cell depending on the expected forces and bandwidths. For larger forces a 10 N load cell is used (Omega Engineering, Model LCFD1KG, www.omega.com), and for small forces a 0.5 N cell (Omega, Model LCFA50G). These cells have four 350 Ω foil strain gauges that are mounted so as to reject off-axis forces and thermal expansion when configured electrically as a full Wheatstone bridge. Both cells displace by roughly 100 micrometers at full load, from which their stiffnesses can be estimated as $5 \times 10^3 \text{ N} \cdot \text{m}^{-1}$ (LCFA50G) and $1 \times 10^5 \text{ N} \cdot \text{m}^{-1}$ (LCFD1KG). The mass of the clamp and shaft that mechanically connect the load cell to the film are 28.8 g and 1.8 g respectively. The LCFA50G 0.5 N cell with the shaft and clamp attached resonates at 23 Hz, as determined from the output power spectrum when the resonance mode is excited. The LCFD1KG 1 kg cell with the shaft and clamp attached is expected to resonate at about 250 Hz, as predicted from the mass and stiffness (frequency = $\text{mass}^{1/2} \cdot \text{stiffness}^{-1/2}$).

The load cells are wired to an instrumentation amplifier (Vishay, Model 2311 Signal Conditioning Amplifier, Raleigh, North Carolina) which provides an excitation voltage of 10 Volts to the strain gauges, balances the bridges, and provides an amplified voltage output proportional to force. The force output can be low-pass filtered with cut-off frequencies of 10 Hz, 100 Hz or 1 kHz.

The load cells are calibrated using a series of known masses. The LCFA50G has a sensitivity of $44.6 \text{ mV}\cdot\text{N}^{-1}$, and the LCFD1KG sensitivity is $1.18 \text{ mV}\cdot\text{N}^{-1}$ at a 10 V excitation.

9.2.6 The Stepping Motor, Controller and Linear Stage

The stepping motor serves to apply displacements to the film in order to maintain constant force. It also provides displacement during passive stress/strain measurements. The stepping motor is a Compumotor 57-51-MO with 200 steps per revolution (www.compumotor.com). It is driven by a Compumotor LN-Drive, set to microstep at 100,000 steps per revolution. The motor drives a New England Affiliated Technologies LM-50 precision linear stage (www.neat.com), with a 50 mm travel, a lead of 2 mm per revolution, a repeatability of 3 μm , and an accuracy of 15 μm .

The drive accepts digital signal inputs for step, direction and power. Each time the step input is pulsed high, the motor is advanced one microstep, producing a displacement of 20 nm. Displacements over long travels are accurate and repeatable to better than 10 μm , as determined by performing twenty consecutive 30 mm displacements, which are measured with a digital calipers having a 10 μm resolution. The films measured are all > 20 mm long, so the applied strain is accurate to better than ± 0.0005 .

9.2.7 Data Acquisition and Output

During isotonic measurements the load cell is used to measure force. The magnitude of the force is an input to a Java program that outputs commands to the stepper motor. The program also computes the applied strain and outputs a signal proportional to strain that is read by the DSA in measuring the strain to current transfer function. A National

Instruments PCI-MIO16XE-10, (www.natinst.com), installed in the PCI slot of the computer, and attached to a breakout board (BNC-2090, www.natinst.com) with BNC connections, provides the analog to digital, A/D, digital to analog, D/A and digital output required. The A/D is configured for ± 10 V inputs, has an input impedance of 100 G Ω in parallel with 100 pF, and samples at up to 100 kHz, at 16 bit resolution (0.15 mV). Similarly the D/A has outputs ± 10 V at up to 100 kHz, at 16-bit resolution (0.15 mV). The digital I/O outputs zero or 5 V at up to 20 MHz.

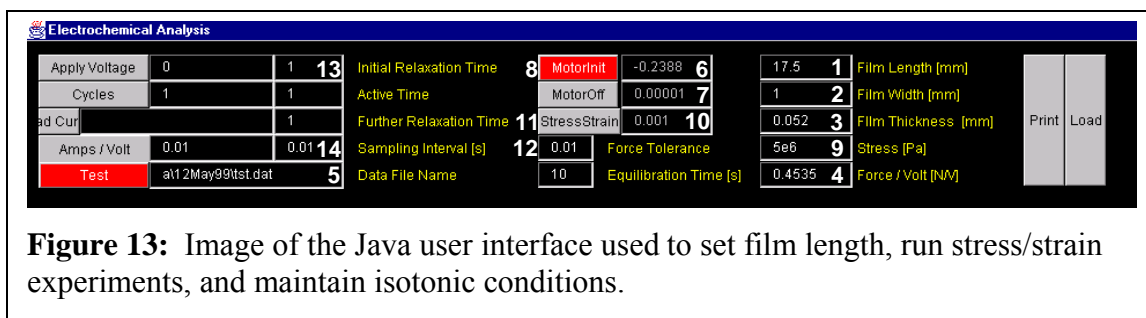


Figure 13: Image of the Java user interface used to set film length, run stress/strain experiments, and maintain isotonic conditions.

9.2.8 The Computer and Graphical User Interface

The computer used to control the applied force is an IBM 6889 PC running Windows NT 4.0 (www.ibm.com). A custom JAVA interface, depicted in Figure 13, is used to control film length in order to maintain constant force on the film, compute and output film strain, and perform stress-strain measurements, recording stress in response to applied strain. It is also used to set film length. The user inputs the measured length in the box indicated by **1** in Figure 13, width in box **2**, and thickness of the film under test in **3**, the force per unit voltage of the load cell/amplifier combination in **4** and the filename to

which any data generated is to be saved in **5**. Commands may then be executed as follows.

9.2.8.1 Applying Film Displacements

Displacements are applied by first specifying the desired displacement in millimeters **6** (Figure 13 label) and the rate in steps per second **7**. Clicking the MotorInit button **8** causes the number of steps necessary to produce the desired displacement to be calculated, and the direction of displacement to be determined. Step commands are then sent to the motor controller via the digital output at time intervals determined by the specified step rate **7**, until the specified displacement **6** is completed. Step commands are sent one step at a time, so the maximum step rate is limited by the closed loop response time of the application/operating system/board, which is 2 ms on average. The maximum strain rate is then $\sim 5 \times 10^{-4} \text{ s}^{-1}$ given the 20 nm per step size.

9.2.8.2 Stress-Strain Measurements

To perform a stress/strain measurement, the change in stress (in Pascals) **9** (label in Figure 13) and the strain rate (in strain per second) **10** are provided by the user. Clicking the StressStrain button **11** leads to a ramp in strain at the specified strain rate **10**. The ramp reverses itself once the maximum stress changes by the set amount **9**, displacing the motor at the same rate in the opposite direction, and over the same number of steps. The film stress is recorded during this cycle. When the ramps are completed, time, strain and stress data are saved in the file name specified **5**.

9.2.8.3 Isotonic Experiments

In order to hold films under isotonic conditions the stress **9** (label in Figure 13), force tolerance **12**, and duration of the experiment in seconds **13** are specified. Clicking the test button causes strain to be ramped at the a prescribed rate **10** until the stress level is reached **9**. Thereafter, until the experiment duration has expired **13**, stress is continuously recorded, and strain is ramped up or down, as is appropriate, until the desired stress level **9** is reached. A step counter is maintained from which net strain is calculated. Time, stress and strain are recorded at specified intervals **14**, and saved to file **5** at the end of the experiment. A voltage proportional to strain is output during the experiment via the D/A, the voltage being updated at the same intervals **14**.

9.3 Measurement Procedures

Films are grown as described in Chapter 4, either on glassy carbon plates or crucibles. They are then cut to 50 mm long, and 2-10 mm wide strips. The dimensions and mass are measured and density is calculated. Resistance is then determined using a four contact probe^{*}, and conductivity is calculated. Films have conductivities in the range of $2\text{-}4.5 \times 10^4 \text{ S}\cdot\text{m}^{-1}$ at room temperature.

Films are then clamped at either end, ready for mounting into the bath, as shown in Figure 2, ensuring that electrical contact is made. The distance between clamps is measured, as is the electrical resistance end to end. Contact resistance is also measured.

^{*} The probe built by Peter Madden, consists of two copper clamps that press films down onto cigarette paper. The clamps are 40 mm apart and provide electrical contact with the film. Two parallel brass sheets, held 25 mm apart by a polyacetal spacer, are placed on the film, with the sheets parallel to the clamps and perpendicular to the film direction. Sense wires are connected to each of the brass sheets, and resistance is measured using an HP3458A multimeter.

The end to end resistance is measured periodically throughout the course of the measurement process, and is found to change by little more than is expected given the gradual increase in dimensions due to film creep.

Concentrations of 0.050 M, 0.30 M and 0.37 M tetraethylammonium hexafluorophosphate in propylene carbonate are prepared. The electrolyte is purged with nitrogen gas for ten minutes and stored under nitrogen until use.

The film and clamps are mounted in the bath, as shown in Figure 3. Stress-strain data are taken. The film is then held under isotonic conditions, typically at 1 MPa, and electrolyte is added to the bath. The reference, counter and working electrodes are connected, with electrical contact being made with the film at both ends. The potentiostat is set to an output voltage equal to the open circuit potential, referred to as the equilibrium potential, V_{eq} . The apparatus is then placed in a glass box in which a constant positive pressure of nitrogen is maintained. Film strain is recorded under isotonic conditions over a period of ten to twenty hours after the addition of electrolyte to determine the extent of swelling. In some cases the admittance is also measured during swelling.

Stress/strain measurements are performed on the film. The film is always pre-stressed to ~3 MPa during these measurements. If the stress-strain relationship is measured from zero force, even slight misalignments of the film leaves portions of the film untensioned, and the stiffness appears non-linear.

Admittance is recorded under isotonic conditions. Otherwise, at constant length, film expansion can lead to buckling and a change in the film to reference distance, which in turn changes the magnitude of the solution resistance. Fixed voltage amplitude, logarithmic swept sine frequency signals are input to the potentiostat by the HP3562A.

The work to reference voltage is input to HP3562A, as is the current, from which the admittance calculated. Typically the voltage amplitude is 0.1 V peak about the equilibrium potential. However, up to 1.4 V are applied to demonstrate linearity and to maximize strain rate.

The solution resistance is found by placing a cylindrical stainless steel probe next to the film under test at various points along the length. The probe consists of a stainless wire shielded by heat shrink, having a total diameter of 1.35 mm. A swept sine is then produced, but instead of recording the reference to film voltage as an input to the Dynamic Signal Analyzer (DSA), the voltage difference between the stainless probe and the reference electrode is recorded. An instrumentation amplifier (Analog Devices BD524 at 10× gain, www.analogdevices.com) is used to increase the effective input impedance of the DSA. The probe has a finite diameter so the resistance between the probe and the surface must be added to the total. Since the probe diameter is small compared with the film width and length, the remaining resistance is calculated from the electrolyte conductivity* ($0.53 \text{ S}\cdot\text{m}^{-1}$ at 0.3 M, $0.13 \text{ S}\cdot\text{m}^{-1}$ at 0.05 M), the film width, length and the probe half diameter, assuming uniform current flow to both sides of the film. Moving the probe along the surface of the film also indicates whether or not there is a potential drop along the length of the film. Such a drop along the film length complicates data interpretation and is not accounted for in the model presented

* The electrolyte conductivity is measured by filling tubing with electrolyte. Stainless steel electrodes are placed at either end of the tubing and the impedance is measured using the HP4194A. The relatively high aspect ratio means that the impedance is purely resistive and constant between 100 Hz and 100 kHz. Conductivity is then easy to calculate given the resistance, and the geometry. (Length is measured and the average cross-sectional area is determined from the distance between electrodes and the mass (volume) of water held within the tube). The result is also compared with the conductivity estimated by comparing the ratio of resistance measured to that obtained from a KCl standard solution.

previously. In the experiments presented, the differences in potential drop as a function of position are less than 10 % of the total drop.

The strain to current transfer function is similarly determined, except that current and strain are the DSA inputs, with voltage being output. The stress to current transfer function is obtained under isometric conditions, with the stress and current being input to the DSA. For all transfer functions the magnitude of the swept sine voltage is changed to ensure that scaling is obeyed and hence the material behavior is dynamically linear.

The transfer functions are plotted in Mathcad 2000 Professional (www.mathsoft.com). The electrical to mechanical efficiency transfer function is calculated from the admittance and strain to charge data.

The diffusive-elastic metal model is then fit to the data. The double layer capacitance, C is calculated using the relationship between it and volumetric capacitance, C_v , obtained from Equations 16 and 18 in Chapter 8, $C_v = C \cdot (\frac{a \cdot C}{2 \cdot k \cdot \epsilon_0 \cdot A} + 1)$, in which the

volumetric capacitance is determined from constant current measurements in Chapter 5 ($7 \cdot 10^7 \text{ F} \cdot \text{m}^{-3}$), k is the dielectric constant of propylene carbonate, ϵ_0 is the permittivity of free space, a is the measured film thickness, and A is the measured surface area. The resistance, R , is the sum of the measured solution resistance, the measured contact resistance and the calculated probe to film resistance. The model admittance is then compared with the data and the diffusion coefficient is adjusted to determine the range of values over which the model curve fits the measured response within experimental error. Strain to charge ratio is obtained by fitting to the measured strain to current transfer function.

9.4 Summary

The apparatus to perform swept sine measurements of admittance, strain to charge and stress to charge of free standing polypyrrole films in tetraethylammonium hexafluorophosphate salt solutions in propylene carbonate have been described. Figures 1, 2 and 3 show the elements of the apparatus used. A model of potentiostat response is also presented in Figure 9, which enables effects of stray capacitance, finite gain, limited input impedance and finite common mode rejection to be distinguished from the electrolyte and film response. Finally, the measurement and model fit procedures have been outlined. In Chapter 10 the results of swept sine analysis are presented, and the diffusive-elastic-metal model is fit to the data.

9.5 Reference List

- Bard, Allen J. and Faulkner, Larry R. *Electrochemical Methods, Fundamentals and Applications*. 1 ed. New York: Wiley; 1980.
- Courtot-Coupez, Jacqueline and L'Her, Maurice. *Electrochimie Dans La Carbonate De Propylene. II. - Domaine D'Electroactivite Et L'Influence De L'Eau*. *Bulletin De La Societe Chimique De France*, 1970, 4, 1631-1636.
- Kohlman, R. S. and Epstein, Arthur J. Insulator-metal transistion and inhomogeneous metallic state in conducting polymers. Skotheim, Terje A.; Elsenbaumer, Ronald L., and Reynolds, John R., Editors. *Handbook of Conducting Polymers*. 2nd ed. New York: Marcel Dekker; 1998; pp. 85-122.